Direct interaction between the Rice yellow mottle virus (RYMV) VPg and the central domain of the Rice eIF(iso)4G1 factor correlates with rice susceptibility and RYMV Virulence

Eugénie Hébrard, Nils Poulicard, Clément Gérard, Oumar Traoré, Hui-Chen Wu, Laurence Albar, Denis Fargette, Yannick Bessin, Florence Vignols

Direct interaction between the *Rice yellow mottle virus* VPg and the central domain of the rice eIF(iso)4G1 factor correlates with rice susceptibility and RYMV virulence

Eugénie Hébrard[1], Nils Poulicard[1], Clément Gérard[2], Oumar Traoré[3], Hui-Chen Wu[4,5], Laurence Albar[4], Denis Fargette[1], Yannick Bessin[2], Florence Vignols[4]

[1]UMR186 Résistance des Plantes aux Bio-agresseurs, Institut de Recherche pour le Développement BP 64501, 34394 Montpellier cedex 5 (France).
[2]UMR5048 Centre de Biochimie Structurale, 29 rue de Navacelles, 34090 Montpellier (France)
[3]Institut de l'Environnement et de Recherches Agricoles (INERA), 01 BP 476, Ouagadougou (Burkina Faso)
[4]UMR5096 Génome et Développement des Plantes, Université de Perpignan via Domitia – CNRS – IRD, BP 64501, 34394 Montpellier cedex 5 (France)
[5]Department of Life Science and Institute of Plant Biology, National Taiwan University, Taipei 10617, Taiwan

Corresponding author: Eugénie Hébrard, e-mail: eugenie.hebrard@ird.fr

ABSTRACT 199 words

The adaptation of *Rice yellow mottle virus* (RYMV) to recessive resistance mediated by the *rymv1-2* allele has been reported as a model to study the emergence and evolution of virulent variants. The resistance and virulence factors have been identified as eukaryotic translation initiation factor eIF(iso)4G1 and Viral Protein genome-linked (VPg), respectively, but the molecular mechanisms involved in their interaction are still unknown. In this study, we demonstrated a direct interaction between RYMV VPg and the central domain of rice eIF(iso)4G1 both *in vitro*, using recombinant proteins, and *in vivo*, using a yeast two-hybrid assay. Insertion of the E309K mutation in eIF(iso)4G1, conferring resistance *in planta*, strongly diminished the interaction with avirulent VPg. The efficiency of the major virulence mutations at restoring the interaction with the resistance protein was assessed. Our results explain the prevalences of virulence mutations fixed during experimental evolution studies and are consistent with the respective viral RNA accumulation levels of avirulent and virulent isolates. Our results also explain the origin of the residual multiplication of wild-type isolates in *rymv1-2*-resistant plants and the role of genetic context in the poor adaptability of the S2/S3 strain. Finally, the strategies of RYMV and *Potyviridae* to overcome recessive resistance were compared.

INTRODUCTION

Plant viruses are important agricultural pathogens worldwide. The use of resistant varieties is the main method of viral disease control. Approximately half of all virus-resistant genes are recessively inherited, whereas resistant genes against other plant pathogens are largely dominant (Kang et al., 2005b). These recessive genes encode plant factors recruited by viral proteins, and resistance mutations in these factors prevent the viral cycle. To date, all cloned recessive resistance genes in crop species encode translation initiation factors (Truniger & Aranda, 2009). Most are resistance genes against *Potyviridae* and encode eIF4E factors. These small host proteins bind the cap structure of mRNA and form part of a multimeric complex that promotes translation initiation (Browning, 2004). The virulence genes have been largely identified as Viral Proteins genome-linked (VPgs). These viral proteins were detected at the 5'end of the viral genomes of several families of viruses (Sadowy et al., 2001). Direct interactions between eIF4Es and VPgs have been previously

demonstrated (Charron et al., 2008, Hwang et al., 2009, Kang et al., 2005a, Leonard et al., 2000, Schaad et al., 2000, Wittmann et al., 1997). The resistant phenotypes result from disruptions of the interactions between eIF4Es and VPgs (Charron et al., 2008, Kang et al., 2005a, Yeam et al., 2007). However, recessive resistance can sometimes be overcome by the emergence of virulent variants (Ayme et al., 2007, Moury et al., 2004). Some virulence mutations in VPgs restore the interactions with proteins encoded by resistance alleles (Charron et al., 2008).

As described above, recessive resistance and virulence factors have been identified, plant and viral mutations have been mapped, and the biochemical roles of these factors have been described in some detail. By contrast, the emergence and evolution of virulent variants in viral populations have been poorly investigated. For most *Potyviridae* studies, data are lacking regarding the mutational pathways that viruses follow, the relationships between these pathways, and the impact of genetic context. However, analyses at both biochemical and population levels should be integrated to better understand virulence acquisition.

Outside the *Potyviridae* family, another biological model has been used to understand the adaptation of viral populations to recessive resistances. *Rice yellow mottle virus* (RYMV) belongs to the unassigned *Sobemovirus* genus. RYMV adaptation to *rymv1-2*–mediated resistance has been previously described. Only two cultivars of the Asiatic rice *Oryza sativa* show a high resistance to RYMV, as characterized by the absence of symptoms and no effect on rice yield (Ndjiondjop et al., 1999, Rakotomalala et al., 2008). The resistance durability of these cultivars has been assessed by experimental evolution, and 15–20% of the isolates were able to overcome this resistance (Fargette et al., 2002, Hébrard et al., 2006, Pinel-Galzi et al., 2007). The virulence factor of RYMV was identified as a VPg (Hébrard et al., 2006, Pinel-Galzi et al., 2007). Parallel evolution of most RYMV strains results in fixation of the same VPg mutations, predominantly at codon 48 (Pinel-Galzi et al., 2007). The virulent variants have been suggested to emerge from a residual multiplication of wild-type isolates in resistant plants, which was estimated by qRT-PCR to be approximately 10^6 viral RNA copies/mg of leaves (Poulicard et al., 2010). The origin of this residual multiplication has not yet been identified. A stepwise optimization of virulent variant fitness by a competition/exclusion phenomenon has been observed (Pinel-Galzi et al., 2007). The conserved site at codon 48, corresponding to an arginine (R) in avirulent isolates, was substituted for different amino acids in virulent isolates. The virulence mutations occurred with contrasted frequencies, and several mutational pathways were followed. In the most prevalent mutational pathway, R48 was displaced by glycine (G) in the first step to become fixed at glutamic acid (E) in the second step. By contrast, the virulence mutation R48I (isoleucine) has been identified as an isolate-specific mutational pathway (Hébrard et al., 2006, Pinel-Galzi et al., 2007). The virulent isolates with the 48E mutation restored the optimal multiplication level of 10^{12} viral RNA copies/mg of leaves in resistant plants, whereas the 48I and 48G mutations induced an intermediate level of accumulation (Poulicard et al., 2010). Increasing affinities between resistance and virulence factors have been proposed to explain the stepwise optimization of virulent variants, but this mechanism remains to be demonstrated (Hébrard et al., 2008).

The viral genetic context influences RYMV adaptability to resistant plants. In contrast to virulent variants, the widely spread West African S2/S3 strain was poorly efficient at overcoming *rymv1-2*–mediated resistance, as more than 98% of S2/S3 isolates failed to evolve toward virulent variants (Pinel-Galzi et al., 2007). S2/S3 virulent variants did not emerge from the main mutational pathway. However, directed mutagenesis to 48I or 48E in a S2/S3 infectious clone could induce virulence. The 48E artificially mutated S2/S3 isolate showed an accumulation rate similar to the S1 strain (Poulicard et al., 2010). Interestingly, artificial mutation to 48G is lethal in the S2/S3 genetic context. In this strain, the main mutational pathway appeared to be blocked at its first step. The codon 49, which is under

diversifying selection, has been previously suggested to be involved in antagonistic epitasis with the codon 48 (Pinel-Galzi et al., 2007).

Although RYMV is a good model for understanding the emergence and evolution of virulent variants in resistant plants, detailed knowledge of the molecular interactions mediating these processes is lacking. The resistance gene *RYMV1* of rice was the only example of a recessive resistance gene from a crop species that does not encode eIF4E (Truniger & Aranda, 2009). *RYMV1* encodes the eukaryotic translation initiation factor eIF(iso)4G1, a scaffold protein that interacts with eIF4E, eIF4A, and the Poly-A binding Protein (PABP) (Albar et al., 2006, Browning, 2004). The *rymv1-2* allele is characterized by an amino acid substitution of glutamic acid (E) to lysine (K) at position 309 of eIF(iso)4G1. However, a direct or indirect interaction between eIF(iso)4G1 and the RYMV VPg has not been demonstrated. In this paper, we investigated (i) the nature of this interaction, (ii) the effects of resistance and virulence mutations on this interaction and (iii) the role of genetic context in the poor adaptability of the S2/S3 strain to *rymv1-2*–mediated resistance. Our results provide a molecular explanation for the frequencies of virulence mutations observed during experimental viral evolution and are consistent with the respective RNA accumulation levels of avirulent and virulent isolates. Furthermore, a residual interaction was detected that could be the source of residual multiplication of wild-type isolates in *rymv1-2*-resistant plants. Negative epistasis in the VPg sequence, which could have explained the genetic constraints observed in the S2/S3 strain, was not observed. Finally, RYMV and potyvirus models were compared.

RESULTS

Structural characterization of the central domain of rice eIF(iso)4G1

The rice resistance gene *RYMV1* has been identified as the eukaryotic translation initiation factor eIF(iso)4G1. Compared to the well-known human eIF4Gs (Lamphear et al., 1995, Marintchev & Wagner, 2005), rice eIF(iso)4G1 is shortened at its two extremities, similar to other plant eIF(iso)4Gs (Figure 1A). The N-terminus of rice eIF(iso)4G1 comprises a conserved eIF4E-interacting domain, a Tyr-X_4-Leu-Leu motif (Mader et al., 1995) and a PolyA binding protein (PABP)-interacting domain, which has not been precisely mapped. The amino acid sequence of the central region of rice eIF(iso)4G1 showed an identity score of 37% with the central domain (named the MIF4G domain) of human eIF4GII, which binds to eIF4A and eIF3. The C-terminus of rice eIF(iso)4G1 showed an identity score of 23% with the human MA3 domain, which contains a second eIF4A-binding site.

We focused on the central domain of rice eIF(iso)4G1 (referred to in this study as MIF4G) because it contains the *rymv1-2* resistance mutation E309K (Albar et al., 2006). The crystal structure of the MIF4G domain of human eIF4GII has been determined, revealing a crescent-like shape with five anti-parallel α-helical hairpins (HEAT-repeats) arranged in a helical stack (Marcotrigiano et al., 2001). Rice MIF4G was previously modeled using the human MIF4G structure as a reference (Albar et al., 2006). The central hairpin also formed helices 3a and 3b but was predicted to be longer than that of human eIF4GII (Figure 1B). It has been suggested that the *rymv1-2* resistance mutation does not affect the MIF4G structure (Albar et al., 2006). To investigate (i) whether the differences between the human eIF4GII and rice MIF4G sequences affect the adoption of the HEAT-repeat conformation and (ii) whether the *rymv1-2* resistance mutation modifies the conformation of the mutated MIF4G (referred to in this study as MIF4G*), we compared the helix contents of rice MIF4G and MIF4G*.

For this purpose, the central region comprising amino acids 206–454 of rice eIF(iso)4G1 was produced as a His-tagged fusion peptide in *E. coli*. The recombinant protein was highly soluble under native conditions and migrated with an apparent and expected

molecular mass of 32 kDa in a 15% SDS-PAGE gel. MIF4G was purified by affinity chromatography in non-denaturing conditions and eluted in one fraction at 11.3 ml by size exclusion chromatography (Figure 2A). In parallel, MIF4G* was produced by inserting the E309K resistance mutation using site-directed mutagenesis. Its expression in *E. coli* led to the production of a recombinant protein exhibiting solubility, electrophoretic properties and purification behavior similar to that of wild-type MIF4G (data not shown). Far-UV circular dichroism (CD) analysis of the purified MIF4G gave a UV spectrum with a maximum at 192 nm and minima at 209 and 222 nm, consistent with the presence of an α-helical conformation (Figure 2B). CD spectra deconvolution carried out with the K2D program (Merelo et al., 1994) indicated a total α-helix content of 37%. These data agreed with the previously published 3D model of rice MIF4G (Albar et al., 2006). The central domain of rice eIF(iso)4G1 forms a putative HEAT-repeat domain. A comparison of wild-type and mutated MIF4Gs by far-UV circular dichroism indicated that the E309K substitution did not induce detectable modifications of the MIF4G structure.

RYMV VPg co-purifies with wild-type MIF4G but not MIF4G* *in vitro*

To test for a physical interaction between RYMV VPg and rice eIF(iso)4G1, we assessed the ability of viral VPg to bind the MIF4G domain in an *in vitro* assay using the recombinant proteins described above. In contrast to MIF4G, production of recombinant RYMV VPg leads to the formation of inclusion bodies (Hébrard et al., 2009). Only a small fraction of the soluble VPg was recovered from the supernatant of a native bacterial protein extract. Moreover, due to its intrinsic disorder tendency, VPg migrated at an apparent mass of 15 and 17 kDa by SDS-PAGE and size exclusion chromatography, respectively, instead of the expected molecular mass of 10.5 kDa (Hébrard et al., 2009). To overcome the technical limitation of poor VPg solubility, a co-purification experiment was performed. A significant increase in VPg solubility was observed in the presence of MIF4G (data not shown). Following purification by Ni^{2+} affinity chromatography, the two proteins eluted in the same fraction during size exclusion chromatography (Figure 3A). This result demonstrates that MIF4G and VPg co-purified in an *in vitro* complex, suggesting a direct binary association of these proteins. It also indicates that the central domain of rice eIF(iso)4G1 is sufficient for co-purification.

We next performed a co-purification experiment of VPg with *rymv1-2*-mutated MIF4G*. The presence of MIF4G* did not increase VPg solubility but instead impaired the ability of the two proteins to co-elute in the same fraction, yielding complete abolition of the *in vitro* interaction between the two proteins (Figure 3B). VPg and MIF4G* eluted in two distinct fractions. The elution volumes corresponded to those observed separately in single purification experiments. This result indicates that the point mutation E309K in MIF4G*, mimicking the *rymv1-2* resistance allele, is sufficient to abolish the *in vitro* interaction with wild-type RYMV VPg.

MIF4G but not MIF4G* strongly interacts with RYMV VPg in a yeast two-hybrid system

The direct interaction between RYMV VPg and MIF4G was further evaluated *in vivo* in a GAL4 yeast two-hybrid system. VPg was constitutively expressed in yeast as a GAL4 DNA-binding domain (DNA-BD) fusion protein from the ADH promoter of the pGBKT7 vector. MIF4G was similarly expressed as a GAL4 activation domain (AD) fusion protein from the pGADT7 plasmid. The yeast strain AH109 was co-transformed with the two plasmids and further spotted as serial dilutions on two different media. The control medium was supplemented with all amino acids and bases to validate uniform growth after transformation. A medium lacking histidine and adenine was used to select yeast cells in

which *in vivo* interactions between selected protein combinations occurred. Figure 4 indicates that co-transformation with VPg- and MIF4G-containing vectors allowed AH109 to grow on the restricted medium lacking adenine and histidine, in contrast to the negative controls (each partner co-transformed with the corresponding empty vector). The interaction was also detected by analyzing LacZ reporter gene transactivation. This result indicates a direct interaction between VPg and MIF4G.

The *rymv1-2* resistance mutation E309K was introduced into pGADT7::MIF4G to precisely assess its impact on the *in vivo* interaction in the yeast two-hybrid system. The interaction of MIF4G* with wild-type VPg was strongly reduced compared to that of wild-type MIF4G (Figure 4), as revealed by the decrease of both the growth in the absence of auxotrophic markers and galactosidase activity. In contrast to the *in vitro* co-purification assay, a residual interaction was detected in yeast. The intensity of yeast growth at an OD_{600} of $5x10^{-2}$ was assessed from 10 independent experiments using ImageJ software, since galactosidase activity was found to be poorly recordable and reliable for weak interactions. After normalization, the interaction between MIF4G* and wild-type VPg was estimated at approximately 15% of the level of the wild-type MIF4G/VPg interaction (Figure 4). This experiment indicated that the yeast two-hybrid system is a sensitive method that allowed us to detect very faint interactions that could not be revealed by co-purification experiments.

Restoration of the interaction with MIF4G* by virulence mutations in RYMV VPg

Similar to the previous experiment, the impact of virulence mutations in VPg on its interaction with MIF4G* was assessed using the yeast two-hybrid assay. For this purpose, virulence mutations were introduced into the pGBKT7::VPg plasmid, creating VPg*. The arginine at position 48 (R48) of wild-type VPg was substituted for either glutamic acid (E), as in the main mutational pathway, or isoleucine (I), as in the isolate-specific mutational pathway. The glycine (G) involved in the first step of the major pathway was also introduced to test its impact on the ability of VPg to interact with MIF4G* in the S2/S3 strain context. The interaction with MIF4G* was restored when the virulence mutations were introduced in VPg (Figure 5). The virulence mutation R48E restored the interaction with MIF4G* to approximately 80% of the level of the wild-type VPg R48/MIF4G interaction (Figure 5). The virulence mutation R48I was less efficient, resulting in an interaction of 20% of the level of the wild-type interaction, which was not significantly different from the residual interaction with wild-type VPg. The virulence mutation R48G, which served to reproduce the S2/S3 strain context when inserted into the pGBKT7::VPg plasmid, induced an intermediate level of restoration of the interaction with mutated MIF4G* (40% of the level of the wild-type interaction). As a control, the interaction between VPg* and wild-type MIF4G was assessed. Each mutated VPg* interacted similarly with wild-type MIF4G (Supplemental Figure 1).

In parallel with the above dot assays, yeast growth was monitored to precisely measure the efficiency and kinetics of each partnership (Figure 6). For this purpose, co-transformed yeast cells were cultured both in a control medium containing all required amino acids and in a medium without adenine, in order to select for yeast two-hybrid interactions. While all double transformants grew similarly in control media, yeast cells producing either wild-type MIF4G/VPg or mutated MIF4G*/VPg*E grew significantly faster than the other cells. Yeast cells producing mutated MIF4G*/VPg*G showed a delay of approximately 10 h in reaching exponential growth, while cells with mutated MIF4G* and VPg*I or wild-type VPg reached exponential growth 30 h later than cells with optimal growth.

DISCUSSION

In this study, *in vitro* co-purification and *in vivo* yeast two-hybrid experiments demonstrated that (1) VPg of RYMV and the central domain of rice eIF(iso)4G1 interact

directly, (2) the *rymv1-2* resistance mutation of MIF4G* strongly diminishes the wild-type VPg interaction, and (3) the VPg virulence mutations restore the MIF4G* interaction with different efficiencies. We provide the first molecular explanation of *rymv1-2*–mediated resistance and RYMV virulence phenotypes, and our results validate our hypothesis of a direct interaction. We propose that, in a compatible interaction, the virus is able to interact with the central domain of eIF(iso)4G1 and complete its infectious cycle. The *rymv1-2* mutation, located in the MIF4G* domain of the eIF(iso)4G1 protein in resistant rice cultivars, strongly decreases the interaction with RYMV VPg, inducing an incompatible interaction and a phenotype of high resistance. However, wild-type VPg can still induce a residual interaction with mutated MIF4G*. We have proposed that this interaction between wild-type VPg and mutated MIF4G*, although limited, is sufficient to permit the residual multiplication of avirulent isolates in resistant plants, which was detected by Q-RT-PCR (Poulicard et al., 2010). Therefore, this limited interaction could be the source of virulence mutations in resistant plants.

Residue–residue contact index preferences, derived from a set of protein–protein interfaces of known structure, have been used to compare predicted affinities along the main mutational pathways to virulence (Hébrard et al., 2008). The highest affinities were predicted to be between E309 of wild-type eIF(iso)4G1 and R48 of wild-type VPg and between K309 of *rymv1-2*-mutated eIF(iso)4G1 and E48 of virulent VPg. Moreover, only the virulent isolate with the R48E mutation has been shown to fully restore optimal virus multiplication in resistant plants (Poulicard et al., 2010). In this study, we demonstrated that the virulent mutation 48E in VPg can restore the optimal interaction with *rymv1-2*-mutated MIF4G* with a higher efficiency than other virulence mutations (48I and 48G). These results explain the contrasted prevalences of virulence mutations observed in experimental evolution and the stepwise fitness optimization process of the main mutational pathway (R/G/E). Furthermore, the major role of residue 48 in VPg in the interaction specificity with MIF4G* might explain the parallel evolution observed in RYMV strains.

The weak ability of the widely spread West African S2/S3 strain to overcome *rymv1-2*–mediated resistance is apparent in experimental evolution studies (Pinel-Galzi et al., 2007). Moreover, artificial insertion of the main virulence mutations 48I, 48G and 48E in an S2/S3 isolate induced contrasted impacts on variant fitness (Poulicard et al., 2010). The virulence mutation 48E induced the same optimal multiplication in resistant plants in both S1 and S2/S3 strain contexts. This was not the case for the virulence mutation 48I, which showed a multiplication rate that was approximately 10^5 times lower when introduced into an S2/S3 than when introduced into an S1 context. In our two-hybrid experiments, the virulence mutation 48I resulted in a weaker restoration of the mutated VPg*/MIF4G* interaction than did 48E. Finally, the virulence mutation 48G was lethal when introduced into the S2/S3 infectious clone. However, we showed an intermediate ability of the VPg 48G two-hybrid construct to restore the interaction with MIF4G*. No antagonistic epistasis was observed in our conditions. This result indicates that the failure of the S2/S3 strain to use the main mutational pathway is not due to an inability of VPg*G to interact with MIF4G*. In the S2/S3 strain context, the 48G mutation may induce a blockage of another function of VPg and/or another step of the viral cycle. Thus, the impact of strain context and genetic constraints on interaction efficiency should be investigated further. Yeast two-hybrid assays are currently being performed to assess the influence of residue 49 under diversifying selection on this interaction. Other resistance alleles have been described that harbor point mutations or short deletions in the central hairpin of MIF4G (Albar et al., 2006). The virulence mutations of these alleles have not yet been identified. The assessment of these resistance and virulence mutations would provide deeper knowledge of the role of each amino acid in the interaction domain.

In this study, we provided the first demonstration for a direct interaction between plant MIF4G and a phytoviral VPg. In order to determine if this strategy is specific to RYMV, the MIF4G interaction ability of VPgs from other viruses should be investigated. A point mutation downstream the MIF4G domain of the eIF4G gene has been associated to the loss of susceptibility of *Arabidopsis thaliana* mutant *cum2* to *Turnip crinkle virus* (genus Carmovirus, family *Tombusviridae*) and *Cucumber mosaic virus (*genus *Cucumovirus,* family *Bromoviridae)* (Yoshii et al., 2004). However, without VPg genes, these viruses must use another strategy to interact with eIF4G. Recently, single nucleotide polymorphisms upstream of the MIF4G domain of the rice eIF4G gene have been associated to the recessive resistance *Rts1* to *Rice tungro spherical virus* (RTSV, genus *Waikavirus,* family *Sequiviridae*) (Lee et al., 2010). Although VPg is detected at the 5' extremity of *Sequiviridae* genome, the VPg domain has not been defined yet. Further studies on *Rts1*-mediated resistance should describe the relationships between RTSV VPg and eIF4G gene. The involvement of eIF4Gs was rarely reported for potyvirus. The incorporation of eIF4G has been shown to strengthen *in vitro* interaction between eIF4E and VPg of *Turnip mosaic virus* (TuMV), *Lettuce mosaic virus* (LMV) and *Potyvirus Y* (Grzela et al., 2006, Michon et al., 2006, Miyoshi et al., 2006). Furthermore, *Arabidopsis thaliana* knock-out mutants for eIF4G and eIF(iso)4G genes lost their susceptibility to LMV, TuMV, *Plum pox virus* and *Clover yellow vein virus* (Nicaise et al., 2007). However, the direct or indirect role of eIF4G during interactions with VPgs remains to be determined. We propose that for *Potyviridae*, the coordinated recruitment of eIF4E/eIF4G or eIF(iso)4E/eIF(iso)4G is an indirect consequence of the direct involvement of the factors 4E and of their interaction specificity with the factors 4G rather than a direct interaction between VPg and factors 4G. Notably, eIF4G is indirectly recruited by *Feline calicivirus* VPgs via interactions with eIF4E (Chaudhry et al., 2006). However, different strategies for eIF recruitments coexist in the same viral family, as demonstrated by the finding that the *Murine norovirus* VPg recruits eIF4G via eIF3 (Chaudhry et al., 2006). Despite their common structural feature of being intrinsically flexible, RYMV VPg does not show sequence homology with caliciviral or potyviral VPgs (Hébrard et al., 2009). Its direct interaction with eIF4G could be another strategy to recruit the translation initiation complex. Although the fact that *Potyviridae* interacts with eIF4Es is well established, the functional relevance of this interaction in translation is still unclear. The role of internal ribosome entry sites in the 5' untranslated regions of the potyviral genomes in supporting translation initiation raised the possibility that VPg has redundant functions (Carrington & Freed, 1990, Levis & Astier-Manifacier, 1993). Other functions in RNA replication and viral movement have been previously suggested (for review, see (Robaglia & Caranta, 2006). Even though the function of eIF recruitment has not yet been determined for *Potyviridae*, the interaction of VPg with MIF4G could play a similar role in RYMV.

MATERIAL AND METHODS

Construction of recombinant proteins

The complete coding sequence of eIF(iso)4G1, obtained from the susceptible *Oryza sativa indica* cultivar IR64, was available in a pGEMT plasmid (Albar et al., 2006). The MIF4G-encoding region was amplified by PCR from the pGEMT::eIF(iso)4G1 construct using the *Bam*HI-containing primers F16 5'-*GGATCC*TTGGTCAGCTAGAAGAGGCA-3' (including MIF4G nucleotides 619-637) and R15 5'-*GGATCC*TTAATCTATTCACGTCGAGGCA-3' (including a sequence complementary to MIF4G nucleotides 1350–1371) and subcloned into the pCR®8/GW/TOPO®TA Cloning® vector (Invitrogen). The *Bam*HI fragment, obtained by digestion of the resulting pCR®8/GW/TOPO®TA::MIF4G construct, was sub-cloned into a pET28 vector at the corresponding *Bam*HI sites as a 6-His N-terminal fusion peptide (Novagen), giving rise to a

pET28::MIF4G construct. Construction of the bacterial expression plasmid pQE60::VPg, corresponding to the RYMV VPg of the isolate CIa (strain S2/S3) with a 6-His C-terminal fusion, was previously described (Hébrard et al., 2009).

To build the yeast two-hybrid plasmids, two subclones, pGEMT::MIF4G and pGEMT::VPg, were constructed to introduce restriction enzyme sites. The MIF4G-encoding region was amplified by PCR using the primers F4G4*Nde*I 5'-CG*CATATG*CCTTGGTCAGCTAGAAGAGG-3' and R4G4*Bam*HI 5'-CG*GGATCC*ATTATTCACGTCGAGGC-3', while the VPg-encoding region was amplified using the primers FVPg*Nde*I 5'-CG*CATATG*TCTCCATTTGAGATTTACGGC-3' and RVPg*Bam*HI 5'-CG*GGATCC*ATTACTCGATATCAACATCC-3'. After digestion, the resulting fragments were cloned into *Nde*I/*Bam*HI–digested pGADT7 and *Nco*I/*Bam*HI–digested pGBKT7, respectively, giving rise to the pGADT7::MIF4G and pGBKT7::VPg constructs.

The pET28::MIF4G*, pGADT7::MIF4G*, pGBKT7::VPg* (with I, G or E substitutions, respectively) vectors carrying MIF4G and VPg variants were obtained by site-directed mutagenesis using the QuikChange Site-Directed Mutagenesis Kit (Stratagene). All primers used in this study are listed in Supplemental Table 1. All constructs were systematically confirmed by sequencing.

Single and co-purification of recombinant proteins

The expression constructs pET28::MIF4G and pET28::MIF4G* were used to separately transform the *E. coli* strain BL21 (DE3) (Novagen). After induction with 0.2 mM isopropyl-1-thio-β-D-galactopyranoside at 37°C for 4 h, cells from 700-ml cultures in LB medium were harvested by centrifugation and frozen at –80°C. Cells were thawed, resuspended in 30 ml of purification buffer (50 mM Tris-HCl, pH 8.0, 300 mM NaCl, 5% glycerol), disrupted with a French press (Thermo) and centrifuged at 18,000 rpm for 30 min. The supernatant was filtered (0.45-µm filters), and purification of MIF4G and MIF4G* under native conditions was carried out using a nickel-loaded HisTrap IMAC HP column (GE Healthcare) followed by gel filtration onto a HR10/300GL Superdex 75 column (GE Healthcare) in 20 mM Tris-HCl, pH 8.0, 300 mM NaCl, and 5% glycerol.

The expression construct pQE60::VPg was used to transform the *E. coli* strain M15-pRep4 (Qiagen) and to produce the recombinant protein at 25°C, as described previously (Hébrard et al., 2009). For co-purification experiments, *E. coli* cultures expressing either MIF4G or VPg were grown independently, and the cell pellets were later mixed together before purification using the protocol mentioned above.

Far-UV circular dichroism

Freshly purified protein samples were used for CD analyses. The sample buffer was changed by eluting the protein from a PD10 desalting column (GE Healthcare) using 10 mM sodium phosphate buffer (pH 8.0) supplemented with 150 mM NaF. After centrifugation, the protein concentration was determined using an ND-1000 Spectrophotometer (NanoDrop Technologies) and an extinction coefficient of 14,000 M^{-1} cm^{-1} for MIF4G and MIF4G*. Far-UV CD spectra were recorded with a Chirascan dichrograph (Applied Photophysics) in a thermostated (20°C) quartz circular cell with a 0.2-mm path length, in steps of 0.5 nm. All protein spectra were corrected by subtracting the respective buffer spectra. The mean molar ellipticity values per residue were calculated using software provided by the manufacturer.

Yeast two-hybrid test

The Matchmaker GAL4 Two-Hybrid System 3 (Clontech Laboratories, Inc.) was used according to the manufacturer's protocols. pGADT7::MIF4G and pGBKT7:VPg constructs

were introduced into the AH109 yeast strain (Clontech). Double-transformed cells were grown on minimal YNB medium (0.7% yeast extract without amino acids, 2% glucose, 2% agar) with all required amino acids including (control) or omitting (Y2H assay) histidine and adenine. Between three and ten clones from four independent transformations were used for the yeast two-hybrid assays. Cells expressing interacting proteins were selected on media lacking leucine and tryptophan (SD-LW) or leucine, tryptophan, histidine, and adenine (SD-LWHA). Cells were grown to stationary phase and adjusted to an OD_{600} of 5.10^{-2}, 5.10^{-3} or 5.10^{-4} before spotting onto the appropriate plates. Plates were incubated at 30°C, and growth was checked 3–5 days after spotting. Empty pGADT7 and pGBKT7 vectors were used as negative controls.

Growth intensities were monitored with ImageJ software (Abramoff et al., 2004), and row data were normalized to positive and negative control and expressed as a percentage of the "initial" interaction between wild-type MIF4G and avirulent VPg. Data were analyzed by ANOVA (Statistica software version 6.0).

The differences in interaction intensities between virulent VPg co-transformants were estimated in an independent experiment. The yeast growth of each co-transformant was kinetically followed as the OD_{600} at 30°C in 10 ml liquid media for 4 days. Two independent experiments were performed with three clones of each construct.

For LacZ assays, transformed AH109 cells (7µL) were plated at 2 OD_{600} on a 3MM Whatmann paper, frozen in liquid nitrogen for 10 seconds and incubated onto a layer paper imbibed with Z buffer containing B-mercaptoethanol and X-Gal as described by AH109 furnisher (Clontech Laboratories, Inc.).

ACKNOWLEDGMENTS

We would like to thank Stelly Mississipi and Christelle Lirette for technical assistance. We are also grateful to N. Declerck, G. Labesse and C. Caranta for helpful discussions and constructive criticisms of the manuscript. This work was partly supported by the Agence Nationale de la Recherche (National project Genoplante, ANR-08-GENM-010). Nils Poulicard was granted a fellowship from the French Ministry of Research.

LITERATURE CITED

Abramoff, M., Magelhaes, P. & Ram, S. (2004). Image Processing with ImageJ. *Biophotonics International* **11**, 36-42.

Albar, L., Bangratz-Reyser, M., Hébrard, E., Ndjiondjop, M., Jones, M. & Ghesquiere, A. (2006). Mutations in the eIF(iso)4G translation initiation factor confer high resistance of rice to *Rice yellow mottle virus*. *Plant Journal* **47**, 417-426.

Ayme, V., Petit-Pierre, J., Souche, S., Palloix, A. & Moury, B. (2007). Molecular dissection of the potato virus Y VPg virulence factor reveals complex adaptations to the pvr2 resistance allelic series in pepper. *Journal of General Virology* **88**, 1594-601.

Browning, K. S. (2004). Plant translation initiation factors: it is not easy to be green. *Biochem Soc Trans* **32**, 589-91.

Carrington, J. C. & Freed, D. D. (1990). Cap-independent enhancement of translation by a plant potyvirus 5' nontranslated region. *Journal of Virology* **64**, 1590-7.

Charron, C., Nicolai, M., Gallois, J. L., Robaglia, C., Moury, B., Palloix, A. & Caranta, C. (2008). Natural variation and functional analyses provide evidence for coevolution between plant eIF4E and potyviral VPg. *Plant Journal* **54**, 56-68.

Chaudhry, Y., Nayak, A., Bordeleau, M. E., Tanaka, J., Pelletier, J., Belsham, G. J., Roberts, L. O. & Goodfellow, I. G. (2006). Caliciviruses Differ in Their Functional

Requirements for eIF4F Components. *Journal of Biological Chemistry* **281**, 25315-25325.
Fargette, D., Pinel, A., Traoré, O., Ghesquière, A. & Konaté, G. (2002). Emergence of resistance-breaking isolates of *Rice yellow mottle virus* during serial inoculations. *European Journal of Plant Pathology* **108**, 585-591.
Grzela, R., Strokovska, L., Andrieu, J.-P., Dublet, B., Zagorski, W. & Chroboczek, J. (2006). Potyvirus terminal protein VPg, effector of host eukaryotic initiation factor eIF4E. *Biochimie* **88**, 887-896.
Hébrard, E., Bessin, Y., Michon, T., Longhi, S., Uversky, V. N., Delalande, F., Dorsselaer, A. V., Romero, P., Walter, J., Declerk, N. & Fargette, D. (2009). Intrinsic disorder in Viral Proteins Genome-Linked: experimental and predictive analyses. *Virology Journal* **6**, e23.
Hébrard, E., Pinel-Galzi, A., Bersoult, A., Siré, C. & Fargette, D. (2006). Emergence of a resistance-breaking isolate of *Rice yellow mottle virus* during serial inoculations is due to a single substitution in the genome-linked viral protein VPg. *Journal of General Virology* **87**, 1369-1373.
Hébrard, E., Pinel-Galzi, A. & Fargette, D. (2008). Virulence domain of the RYMV Genome-Linked Viral Protein VPg towards rice rymv1-2-mediated resistance. *Archives of Virology* **153**, 1161-1164.
Hwang, J., Li, J., Liu, W. Y., An, S. J., Cho, H., Her, N. H., Yeam, I., Kim, D. & Kang, B. C. (2009). Double mutations in eIF4E and eIFiso4E confer recessive resistance to Chilli veinal mottle virus in pepper. *Molecules and Cells* **27**, 329-36.
Kang, B. C., Yeam, I., Frantz, J. D., Murphy, J. F. & Jahn, M. M. (2005a). The pvr1 locus in Capsicum encodes a translation initiation factor eIF4E that interacts with Tobacco etch virus VPg. *Plant Journal* **42**, 392-405.
Kang, B. C., Yeam, I. & Jahn, M. M. (2005b). Genetics of plant virus resistance. *Annu Rev Phytopathol* **43**, 581-621.
Lamphear, B. J., Kirchweger, R., Skern, T. & Rhoads, R. E. (1995). Mapping of functional domains in eukaryotic protein synthesis initiation factor 4G (eIF4G) with picornaviral proteases. Implications for cap-dependent and cap-independent translational initiation. *Journal of Biological Chemistry* **270**, 21975-83.
Lee, J.-H., Muhsin, M., Atienza, G. A., Kwak, D.-Y., Kim, S.-M., De Leon, T. B., Angeles, E. R., Coloquio, E., Kondoh, H., Satoh, K., Cabunagan, R. C., Cabauatan, P. Q., Kikuchi, S., Leung, H. & Choi, I.-R. (2010). Single Nucleotide Polymorphisms in a Gene for Translation Initiation Factor (eIF4G) of Rice (Oryza sativa) Associated with Resistance to Rice tungro spherical virus. *Molecular Plant-Microbe Interactions* **23**, 29-38.
Leonard, S., Plante, D., Wittmann, S., Daigneault, N., Fortin, M. G. & Laliberte, J. F. (2000). Complex formation between potyvirus VPg and translation eukaryotic initiation factor 4E correlates with virus infectivity. *Journal of Virology* **74**, 7730-7737.
Levis, C. & Astier-Manifacier, S. (1993). The 5' untranslated region of PVY RNA, even located in an internal position, enables initiation of translation. *Virus Genes* **7**, 367-79.
Mader, S., Lee, H., Pause, A. & Sonenberg, N. (1995). The translation initiation factor eIF-4E binds to a common motif shared by the translation factor eIF-4 gamma and the translational repressors 4E-binding proteins. *Molecular and Cellular Biology* **15**, 4990-7.
Marcotrigiano, J., Lomakin, I. B., Sonenberg, N., Pestova, T. V., Hellen, C. U. & Burley, S. K. (2001). A conserved HEAT domain within eIF4G directs assembly of the translation initiation machinery. *Molecular Cell* **7**, 193-203.

Marintchev, A. & Wagner, G. (2005). eIF4G and CBP80 share a common origin and similar domain organization: implications for the structure and function of eIF4G. *Biochemistry* **44**, 12265-72.

Merelo, J. J., Andrade, M. A., Prieto, A. & Morán, F. (1994). Proteinotopic Feature Maps. *Neurocomputing* **6**, 443-454.

Michon, T., Estevez, Y., Walter, J., German-Retana, S. & Le Gall, O. (2006). The potyviral virus genome-linked protein VPg forms a ternary complex with the eukaryotic initiation factors eIF4E and eIF4G and reduces eIF4E affinity for a mRNA cap analogue. *FEBS J* **273**, 1312-1322.

Miyoshi, H., Suehiro, N., Tomoo, K., Muto, S., Takahashi, T., Tsukamoto, T., Ohmori, T. & Natsuaki, T. (2006). Binding analyses for the interaction between plant virus genome-linked protein (VPg) and plant translational initiation factors. *Biochimie* **88**, 329-40.

Moury, B., Morel, C., Johansen, E., Guilbaud, L., Souche, S., Ayme, V., Caranta, C., Palloix, A. & Jacquemond, M. (2004). Mutations in *Potato virus Y* genome-linked protein determine virulence toward recessive resistances in *Capsicum annuum* and *Lycopersicon hirsutum*. *Molecular Plant Microbe Interactions* **17**, 322-329.

Ndjiondjop, M. N., Albar, L., Fargette, D., Fauquet, C. & Ghesquière, A. (1999). The genetic basis of high resistance to rice yellow mottle virus (RYMV) in cultivars of two cultivated rice species. *Plant Disease* **83**, 931-935.

Nicaise, V., Gallois, J. L., Chafiai, F., Allen, L. M., Schurdi-Levraud, V., Browning, K. S., Candresse, T., Caranta, C., Le Gall, O. & German-Retana, S. (2007). Coordinated and selective recruitment of eIF4E and eIF4G factors for potyvirus infection in Arabidopsis thaliana. *FEBS Letters* **581**, 1041-1046.

Pinel-Galzi, A., Rakotomalala, M., Sangu, E., Sorho, F., Kanyeka, Z., Traoré, O., Sérémé, D., Poulicard, N., Rabenantaondro, Y., Séré, Y., Konaté, G., Ghesquière, A., Hébrard, E. & Fargette, D. (2007). Theme and variations in the evolutionary pathways to virulence of an RNA plant virus species. *PLoS Pathogens* **3**, e180.

Poulicard, N., Pinel-Galzi, A., Hébrard, E. & Fargette, D. (2010). Why Rice yellow mottle virus, a rapidly evolving RNA plant virus, is not efficient at breaking rymv1-2 resistance. *Molecular Plant Pathology* **11**, 145–154.

Rakotomalala, M., Pinel-Galzi, A., Albar, L., Ghesquière, A., Ramavovololona, P., Rabenantaondro, Y. & Fargette, D. (2008). Resistance to Rice yellow mottle virus in the rice germplasm in Madagascar. *European Journal of Plant Pathology*.

Robaglia, C. & Caranta, C. (2006). Translation initiation factors: a weak link in plant RNA virus infection. *Trends in Plant Science* **11**, 40-45.

Sadowy, E., Milner, M. & Haenni, A. L. (2001). Proteins attached to viral genomes are multifunctional. *Adv Virus Res* **57**, 185-262.

Schaad, M. C., Anderberg, R. J. & Carrington, J. C. (2000). Strain-specific interaction of the tobacco etch virus NIa protein with the translation initiation factor eIF4E in the yeast two-hybrid system. *Virology* **273**, 300-306.

Truniger, V. & Aranda, M. A. (2009). Recessive resistance to plant viruses. *Adv Virus Res* **75**, 119-59.

Wittmann, S., Chatel, H., Fortin, M. G. & Laliberte, J. F. (1997). Interaction of the viral protein genome linked of *Turnip mosaic potyvirus* with the translational eukaryotic initiation factor (iso) 4E of *Arabidopsis thaliana* using the yeast two-hybrid system. *Virology* **234**, 84-92.

Yeam, I., Cavatorta, J. R., Ripoll, D. R., Kang, B. C. & Jahn, M. M. (2007). Functional dissection of naturally occurring amino acid substitutions in eIF4E that confers recessive potyvirus resistance in plants. *Plant Cell* **19**, 2913-2928.

Yoshii, M., Nishikiori, M., Tomita, K., Yoshioka, N., Kozuka, R., Naito, S. & Ishikawa, M. (2004). The Arabidopsis cucumovirus multiplication 1 and 2 loci encode translation initiation factors 4E and 4G. *Journal of Virology* **78**, 6102-6111.

Figure 1: Organization of the MIF4G central domain of rice eIF(iso)4G1. (A) Human eIF4GII is a modular protein containing three regions separated by flexible hinges. The N-terminal region contains the binding site for PABP and the eIF4E-binding motif Y-X4-L-L. The MIF4G central region of eIF4GII binds to eIF4A and eIF3. The C-terminal domain comprises the MA3 and W2 domains. The MA3 domain carries a second eIF4A-binding site. The W2 domain, also called an AA (acidic/aromatic) box–containing repeat, binds to MAP kinase–interacting kinases. Shorter than human eIF4GII, rice eIF(iso)4G1 has a length of 806 aa and lacks the PABP-containing N-terminal and W2-containing C-terminal extensions. Conserved domains are colored black. They include the conserved eIF4E-interacting domain and an amino acid sequence sharing 37% and 23% identity with the human MIF4G and MA3 domains, respectively. (B) The modeled structure of rice MIF4G is similar to the published structure of human MIF4G, as indicated by the predicted and observed α-helices, denoted by gray cylinders. The longer helices 3a and 3b in rice MIF4G encompass the resistance mutations, denoted by hatched squares.

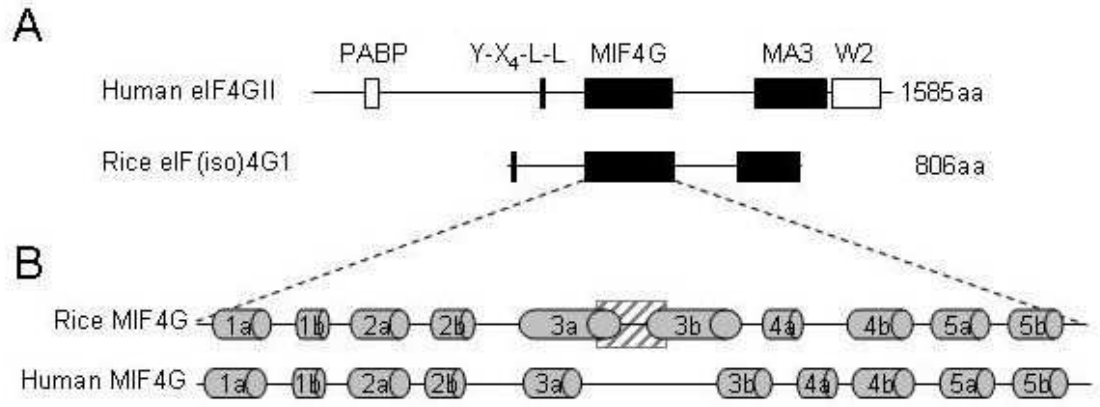

Figure 2: The MIF4G central domain of rice eIF(iso)4G1 adopts an α-helical conformation. (A) Recombinant His-tagged rice MIF4G was purified by affinity chromatography. Purified His-tagged rice MIF4G was eluted in one fraction from a Superdex 75 HR10/30 column (GE Healthcare) in 50 mM Tris-HCl, pH 8, and 300 mM NaCl, at a flow rate of 0.5 ml/min (F1) (inset: 15% SDS-PAGE). (B) The far-UV circular dichroism spectra show characteristic maxima at 192 nm and minima at 209 and 222 nm, confirming the presence of an α-helical conformation. Site-directed mutagenesis was used to introduce an E309K point mutation, mimicking the *rymv1-2* resistance allele, into the His-tagged MIF4G construct. The spectra of rice MIF4G and MIF4G* are similar. The E309K mutation induced no conformational changes in the MIF4G domain.

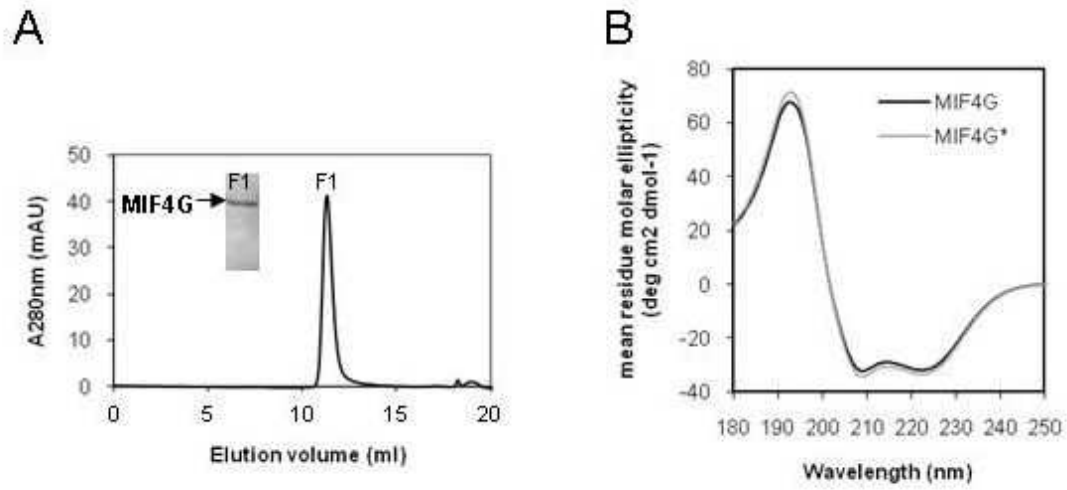

Figure 3: The viral VPg protein interacts *in vitro* with MIF4G but not with *rymv1-2*-mutated MIF4G* in a co-purification assay. Both MIF4G or MIF4G* and VPg recombinant proteins were loaded and co-purified from a Superdex 75 HR10/30 column with an elution buffer containing 50 mM Tris-HCl, pH 8, and 300 mM NaCl, at a flow rate of 0.5 ml/min. (A) With wild-type MIF4G, the elution profile shows the presence of the two proteins in one unique fraction, F1 (inset: 15% SDS-PAGE). (B) With MIF4G*, the elution profile shows the presence of MIF4G* and VPg in distinct fractions, F1 and F2 (inset: 15% SDS-PAGE).

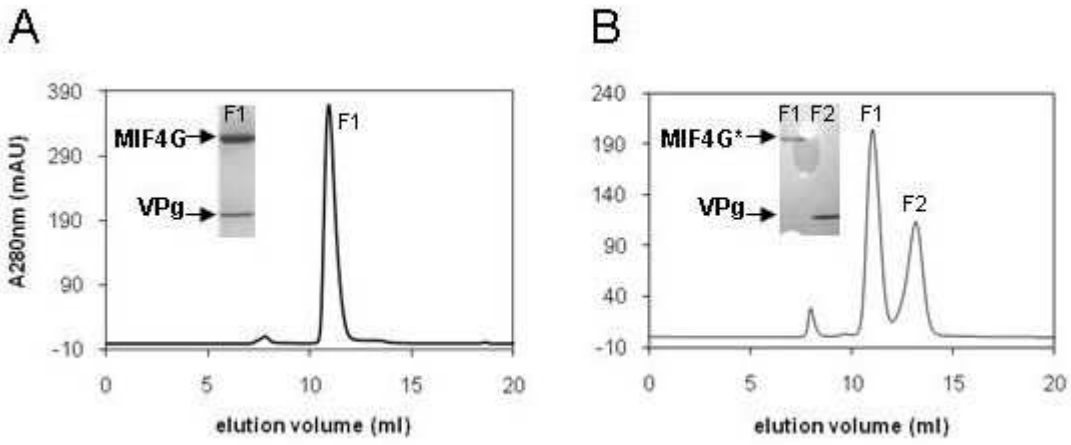

Figure 4: Wild-type MIF4G and *rymv1-2*-mutated MIF4G* interact differently with the viral VPg protein in a yeast two-hybrid assay. Site-directed mutagenesis was used to introduce an E309K point mutation, mimicking the *rymv1-2* resistance allele, into the pGAD::MIF4G construct. The yeast strain AH109 was co-transformed with either pGAD::MIF4G or pGAD::MIF4G* and pGBK::VPg constructs or with a set of negative controls (empty pGAD/empty pGBK, empty pGAD/pGBK::VPg and pGAD::MIF4G/empty pGBK). Cells were plated as serial dilutions (OD_{600} of $5x10^{-2}$, $5x10^{-3}$ and $5x10^{-4}$) on a control plate with (first panel) or without (second panel) the histidine amino acid and the adenine base. Yeast cells were allowed to grow at 30°C for 4 days. Neither the pGAD::MIF4G/empty pGBK nor the pGBK::VPg/empty pGAD pairs of constructs allowed yeast growth on selective media without histidine and adenine, indicating the absence of autonomous activation of the reporter genes ADE2 and HIS3 by MIF4G or VPg. A direct interaction between VPg and MIF4G was demonstrated as indicated by the ability of the co-transformed yeast cells to grow in the absence of histidine and adenine. By contrast, the VPg interaction was strongly reduced by the E309K substitution. Interactions were also recorded by their ability to transactivate the LacZ reporter gene (third panel). The direct interaction between VPg and MIF4G is visualized as a strong blue staining due to LacZ transactivation. The VPg/MIF4G interaction is reduced by the E309K substitution in MIF4G as revealed by a light blue staining. No galactosidase activity is detected in cells co-transformed by negative control constructs. Because precise LacZ activity was hardly measurable due to the weakness of some interactions, comparisons of yeast growth were estimated as percentages after quantifying spot intensities presented on second panel using ImageJ (fourth panel), with 100% control efficiency being assigned to the susceptible MIF4G/VPg binary interaction. a, b, c, represent groups significantly different after multiple mean comparison (ANOVA, P = 0.05). Results were highly reproducible and are the means of 10 independent experiments.

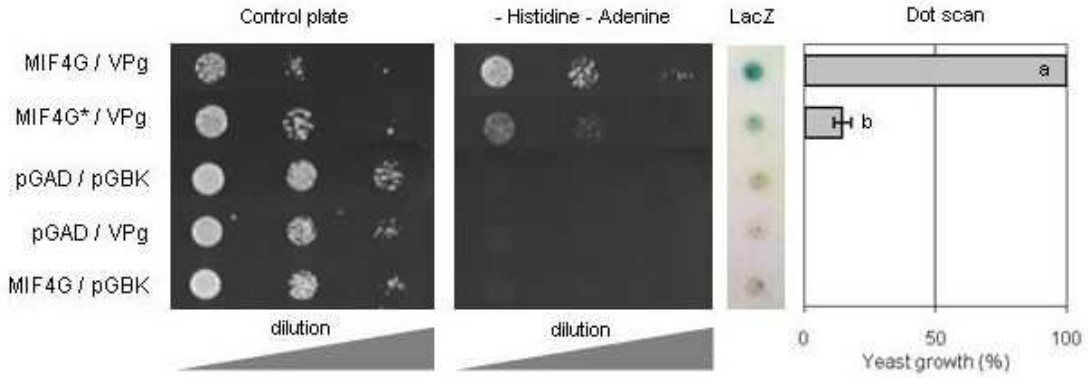

Figure 5: Point mutations at residue R48, mimicking virulent VPgs, restore *in vivo* interactions between VPg and *rymv1-2*-mutated MIF4G*. Site-directed mutagenesis was used to introduce R48I, R48G and R48E point mutations into the pGBK::VPg construct. These constructs were used to transform the AH109 yeast strain together with the pGAD::MIF4G* construct. Transformed yeast cells were cultured as described in Figure 4. The interaction strength between VPg and MIF4G* was successively reinforced by virulence mutations in VPg (VPg*I to VPg*E), as visualized by dot assays (middle panels) and growth percentage comparisons (fourth panel). While the MIF4G*/VPg interaction was only 10% of the strength of the control interaction, the highest interaction score was obtained for the virulence mutation R48E, which restored the interaction with MIF4G* to approximately 80% of the wild-type efficiency. Inversely, the lowest interaction score was obtained with the virulence mutation R48I (MIF4G*/VPg*I), which interacted at only 20% of the strength of the MIF4G/VPg control interaction. The virulence mutation R48G induced an intermediate interaction strength of 40% of the strength of the control interaction. Interactions are also recorded by their ability to transactivate the LacZ reporter gene (third panel) and by ImageJ scanning (fourth panel) as described in Figure 4. Results represent the means of 10 independent experiments.

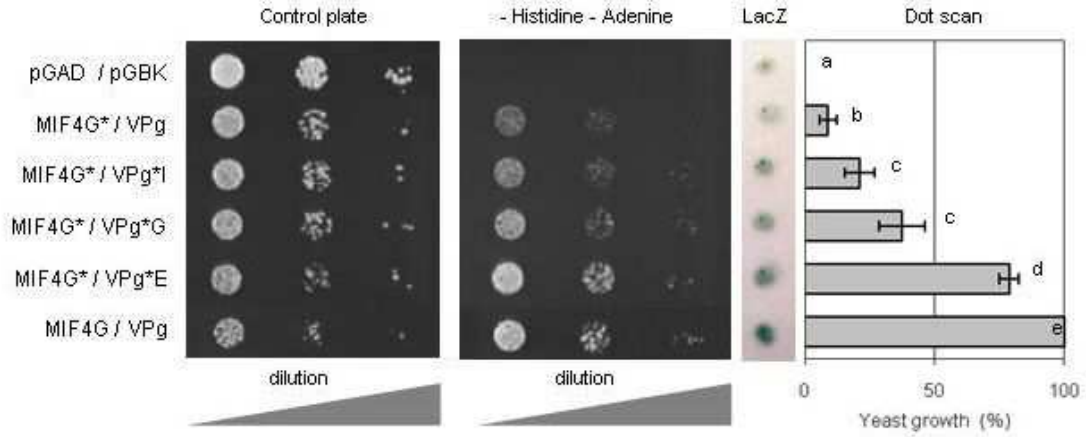

Figure 6: Time course of co-transformed yeast growth in control or selective liquid medium. The growth rates of cells that were co-transformed as described in Figure 5 were monitored by OD_{600} measurements of liquid cultures either containing all required amino acids, for proper growth in the absence of an interaction (left panel), or lacking adenine, to select for an interaction (right panel). While all co-transformed cells grew similarly in the control medium, cells producing susceptible MIF4G/avirulent VPg and resistant MIF4G*/virulent VPg*E partner proteins grew faster than the other cells, and cells producing resistant MIF4G*/virulent VPg*G showed a 10-h delay in reaching exponential growth. Cells carrying resistant MIF4G* and virulent VPg*I or avirulent VPg exhibited a 30-h delay in reaching the optimal growth. Values represent the means of three individual cells per pair of partners and from two independent transformation events.

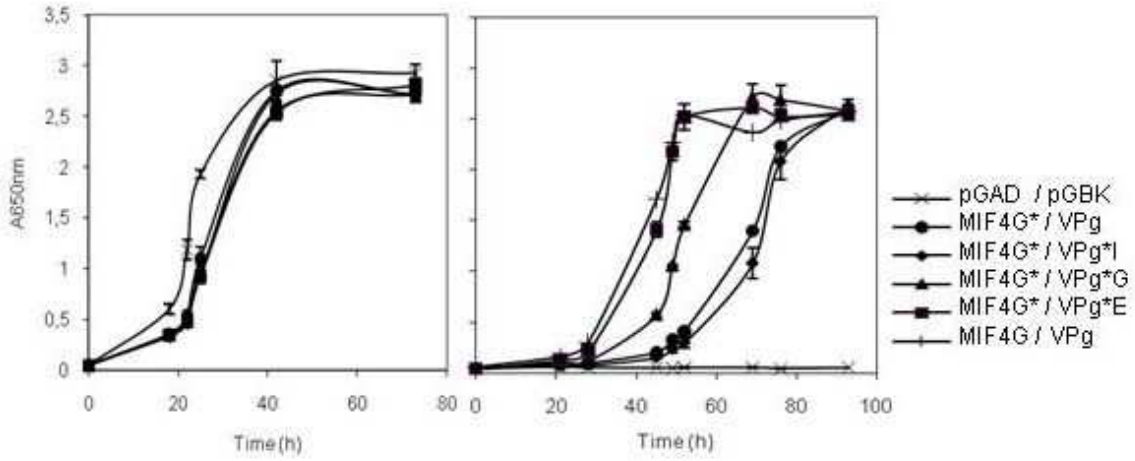

Supplemental data

Table S1: List of primers used for site-directed mutagenesis

FMIFE309K	5' GCTGAGAGCCTAAGGGCTAAAATAGCAAAATTGACTGG 3'
RMIFE309K	5' CCAGTCAATTTTGCTATTTTAGCCCTTAGGCTCTCAGC 3'
FVPgR48I	5' CTGGGTGCGTGAGATAACGAAGTACCACGCTGAG 3'
RVPgR48I	5' CTCAGCGTGGTACTTCGTTATCTCACGCACCCAG 3'
FVPgR48G	5' GGGTGCGTGAGGGAACGAAGTACCACGCTGAG 3'
RVPgR48G	5' CTCAGCGTGGTACTTCGTTCCCTCACGCACCC 3'
FVPgR48E	5' CTGGGTGCGTGAGGAAACGAAGTACCACGCTGAGG 3'
RVPgR48E	5' CCTCAGCGTGGTACTTCGTTTCCTCACGCACCCAG 3'

Figure S1: Point mutations at residue R48, mimicking virulent VPgs, interact with wild-type MIF4G. VPg mutants mimicking virulent isoforms at residue R48 that interacted with wild-type MIF4G constructs were used to transform the AH109 yeast strain together with the pGAD::MIF4G construct. Interaction strength values between virulent VPgs and wild-type MIF4G were similar and were approximately 70–80% of control interaction values, as visualized by dot assays (middle panel) and growth percentage comparisons (right panel).